

TEXES OBSERVATIONS OF PURE ROTATIONAL H₂ EMISSION FROM AB AURIGAE

MARTIN A. BITNER^{1,2}, MATTHEW J. RICHTER^{2,3}, JOHN H. LACY^{1,2}, THOMAS K. GREATHOUSE^{2,4}, DANIEL T. JAFFE^{1,2},
GEOFFREY A. BLAKE⁵

Draft version November 20, 2021

ABSTRACT

We present observations of pure rotational molecular hydrogen emission from the Herbig Ae star, AB Aurigae. Our observations were made using the Texas Echelon Cross Echelle Spectrograph (TEXES) at the NASA Infrared Telescope Facility and the Gemini North Observatory. We searched for H₂ emission in the S(1), S(2), and S(4) lines at high spectral resolution and detected all three. By fitting a simple model for the emission in the three transitions, we derive $T = 670 \pm 40$ K and $M = 0.52 \pm 0.15 M_{\oplus}$ for the emitting gas. Based on the 8.5 km s^{-1} FWHM of the S(2) line, assuming the emission comes from the circumstellar disk, and with an inclination estimate of the AB Aur system taken from the literature, we place the location for the emission near 18 AU. Comparison of our derived temperature to a disk structure model suggests that UV and X-ray heating are important in heating the disk atmosphere.

Subject headings: circumstellar matter, infrared:stars, stars:planetary systems, protoplanetary disks, stars:individual(AB Aur), stars:pre-main sequence

1. INTRODUCTION

Disks around young stars are a natural part of the star formation process and, as the likely site of planet formation, have generated much interest. A considerable amount has been learned about the structure of circumstellar disks through the study of dust emission and detailed modeling of the spectral energy distributions (SED) of these stars. However, if we assume the standard gas-to-dust ratio for the interstellar medium, dust makes up only 1% of the mass of the disk. Thus there is an interest in developing direct tracers of the gas component. Studies of gas in disks have so far focused mainly on gas at either large radii (> 50 AU), using observations at submillimeter wavelengths (Semenov et al. 2005), or small radii, using observations of near-infrared CO lines (Blake & Boogert 2004; Najita et al. 2003). Mid-infrared spectral diagnostics may probe disks at intermediate radii (1-10 AU) (Najita et al. 2006).

Molecular hydrogen diagnostics are promising because they trace the dominant constituent of the disk and so do not rely on conversion factors to determine the mass of the emitting gas. H₂ has been observed in circumstellar environments at ultraviolet (Johns-Krull et al. 2000) and near-infrared (Bary et al. 2003) wavelengths. These observations trace hot circumstellar gas, or gas excited by fluorescent processes, and are therefore difficult to trans-

late into gas masses. The pure rotational mid-infrared H₂ lines are useful probes because the level populations should be in LTE at the local gas temperature, and so line ratios allow determination of the excitation temperature and mass of the warm gas. The line ratios of the three low-J lines accessible from the ground are sensitive to gas at temperatures of 200-800 K. Other lines in the mid-infrared such as [NeII] at $12.8 \mu\text{m}$ (Glassgold et al. 2007), [SI] at $25.2 \mu\text{m}$ and [FeII] at $26 \mu\text{m}$ (Pascucci et al. 2006) should be useful probes of gas in disks but their interpretation requires detailed modeling. Molecular hydrogen emission does not trace the cold, optically thick regions of disks, and therefore estimates of the amount of warm gas based on H₂ emission represent a lower limit to the total disk mass. In order to see H₂ emission arising from a disk, the warm gas must be either physically separated from optically thick dust or at a different temperature. These conditions can be met in the disk surface layer or in gaps or holes in the disk. In either case, gas can be physically separated (due to dust settling or clearing) as well as thermally decoupled (due to lower densities) from the dust and heated to a higher temperature by X-ray and UV radiation (Glassgold et al. 2004; Gorti & Hollenbach 2004; Nomura & Millar 2005).

From the ground, three H₂ mid-infrared rotational lines are accessible: S(1) ($\lambda = 17.035 \mu\text{m}$), S(2) ($\lambda = 12.279 \mu\text{m}$), and S(4) ($\lambda = 8.025 \mu\text{m}$). The high spectral resolution achievable with the Texas Echelon Cross Echelle Spectrograph (TEXES; Lacy et al. 2002) is crucial for these observations in order to separate the lines from nearby telluric features and to maximize the line contrast against the dust continuum. Observations at high spectral resolution also have the advantage that, when coupled with information about the disk inclination, they allow an estimate for the location of the emitting gas. For emission lines with small equivalent width, ground-based observations with TEXES can be more sensitive than *Spitzer* IRS observations.

AB Aur is one of the brightest and thus one of the most well-studied of the Herbig Ae stars. It is located

arXiv:0704.1481v1 [astro-ph] 11 Apr 2007

¹ Department of Astronomy, University of Texas at Austin, Austin, TX 78712; mbitner@astro.as.utexas.edu, lacy@astro.as.utexas.edu, dtj@astro.as.utexas.edu

² Visiting Astronomer at the Infrared Telescope Facility, which is operated by the University of Hawaii under Cooperative Agreement no. NCC 5-538 with the National Aeronautics and Space Administration, Science Mission Directorate, Planetary Astronomy Program.

³ Physics Department, University of California at Davis, Davis, CA 95616; richter@physics.davis.edu

⁴ Lunar and Planetary Institute, Houston, TX 77058; greathouse@lpi.usra.edu

⁵ Division of Geological & Planetary Sciences, California Institute of Technology, MS 150-21, Pasadena, CA 91125; gab@gps.caltech.edu

at a distance of 144 pc based on Hipparcos measurements (van den Ancker et al. 1998), has a spectral type of A0-A1 (Hernández et al. 2004) and is surrounded by a disk/envelope structure that extends to at least $r \sim 450$ AU (Mannings & Sargent 1997). Observations at 11.7 and 18.7 μm by Chen & Jura (2003) show that AB Aur varies in the mid-infrared. The mass of the star is $2.4 M_{\odot}$ with an age of 2-4 Myr (van den Ancker et al. 1998). AB Aur has a SED which is well-fit by the passive irradiated disk with puffed-up inner rim model of Dullemond et al. (2001). There have been a wide range of inclination estimates for AB Aur (see Brittain et al. 2003 for an extended discussion of this issue). Recent results by Semenov et al. (2005) derive an inclination of 17^{+6}_{-3} deg for the AB Aur system by modeling millimeter observations. We will assume this value for analysis of our data.

Several attempts have been made to observe molecular hydrogen emission from the disk of AB Aur. Thi et al. (2001) claimed the detection of H_2 S(0) and S(1) emission associated with the AB Aur system using the *Infrared Space Observatory (ISO)*, but subsequent observations from the ground with improved spatial resolution were unable to confirm the emission (Richter et al. 2002). Richter et al. (2002) and Sheret et al. (2003) saw some evidence of emission in the S(2) line but the data quality was such that a definitive statement could not be made. They saw no evidence of the S(1) line. In this paper, we present definite detections of the S(1), S(2), and S(4) lines.

2. OBSERVATIONS AND DATA REDUCTION

All of the data were acquired using TEXES in its high-resolution mode on the NASA Infrared Telescope Facility (IRTF) between December 2002 and October 2004 and on Gemini North in November 2006 under program ID GN-2006B-Q-42. Table 1 lists details of the observations. We nodded the source along the slit to remove background sky emission. We observed flux and telluric standards at each setting. Other calibration files taken include blank sky and an ambient temperature blackbody used to calibrate the wavelength and to flatfield the data.

The data were reduced using the standard TEXES pipeline (Lacy et al. 2002) which produces wavelength-calibrated one dimensional spectra. The TEXES pipeline data reduction gives a first order flux calibration. However, because of the different slit illumination of the ambient temperature blackbody and point sources, we observed flux standards to determine a correction factor. We assumed that the slit illumination was the same for the target as for the flux standard. Guiding and seeing variations can introduce uncertainty into our flux calibration.

3. RESULTS

Figure 1 shows flux-calibrated spectra for all three settings taken at the Gemini North Observatory. Overplotted on each spectrum is a Gaussian with integrated line flux equal to that derived from the best-fit model assuming the emission arises from an isothermal mass of optically thin H_2 gas. The three lines were fit simultaneously while varying the temperature and mass of the emitting gas in the model. For the simultaneous fitting, we adopted the FWHM and centroid of the S(2) line for

all three lines. The quoted errors for the temperature and mass are $1\text{-}\sigma$ based on the contour plot of the χ^2 values. Our best-fit model based on Gemini data has $T = 670 \pm 40$ K and $M = 0.52 \pm 0.15 M_{\oplus}$. A similar analysis of our IRTF data, which consisted of a detection at S(2) and upper limits for S(1) and S(4), gives $T = 630 \pm 60$ K and $M = 0.7 \pm 0.2 M_{\oplus}$. Though within $2\text{-}\sigma$ uncertainties, the lower measured S(2) flux observed at Gemini than from the IRTF combined with the fact that our slit is smaller on the sky at Gemini suggests we may be resolving out some of the flux we see at the IRTF. To investigate this possibility, we examined spatial plots of our 2-D echellograms but found no clear evidence for the existence of spatially resolved line emission.

Table 2 contains a summary of our results. We fit each line individually with a Gaussian to determine centroid, FWHM, and flux values. The lines are all centered near the systemic velocity of AB Aur and have FWHM ~ 10 km s^{-1} . Roberge et al. (2001) find $A_v = 0.25$ for AB Aur, so we assume no extinction at our wavelengths. We quote equivalent widths in addition to line fluxes due to uncertainty in the determination of the continuum level. In an attempt to test how sensitive our temperature and mass estimates are to errors in the flux calibration, we fit our data after normalizing to the continuum flux values from ISO SWS observations of AB Aur (Meeus et al. 2001). The resulting temperature and mass do not differ significantly from the values based on our internal flux calibration. We derive $T = 630$ K and $M = 0.71 M_{\oplus}$ when normalizing to the ISO continuum values of 13.1 Jy at 8 μm , 21.0 Jy at 12 μm , and 30.8 Jy at 17 μm before fitting. The upper limits for S(1) and S(4) from the IRTF quoted in Table 2 are based on a Gaussian fit at the expected position of each line plus a $1\text{-}\sigma$ error. The $1\text{-}\sigma$ line flux errors were computed by summing over the number of pixels corresponding to the FWHM of the lines in regions of the spectrum with similar atmospheric transmission.

Figure 2 shows a population diagram based on our observations. The points marked are based on the line fluxes derived from Gemini observations listed in Table 2, and the error bars are $1\text{-}\sigma$. The overplotted solid line is not a fit to the population diagram; rather it is based on the best-fit model temperature and mass. Even though we only have three points, the deviation from a single temperature (a straight line on this plot) is significant and may indicate that the emission is coming from a mix of temperatures, as expected for a disk with a radial temperature gradient. We note that curvature in the population diagram can also occur if the ortho-to-para (OTP) ratio is different from our assumed value of 3. Fuente et al. (1999) derived a an OTP ratio between 1.5-2 for H_2 in a photodissociation region with gas temperatures of 300-700 K. However, the sense of the curvature in our population diagram would require an OTP ratio greater than 3 to explain the increased S(1) flux, which seems unlikely. We discuss the derived temperature of the gas and its location in the next section.

4. DISCUSSION

We have detected all three mid-IR H_2 lines with good signal to noise. The results are consistent with the previous upper limits and the $2\text{-}\sigma$ detection of the S(2) line (Richter et al. 2002; Sheret et al. 2003). Our observations

of all three lines allow us to put tighter constraints on the temperature and mass of the emitting gas. The analysis of our data has three components. First, we determine a characteristic temperature of the emitting gas by fitting a simple model to the three lines. Second, we locate the position in the disk where the emission arises by comparing our observed line profiles to line profiles calculated from a Keplerian disk model. Finally, in order to comment on the structure of the disk, we compare our results to the predictions of a well-established disk structure model which assumes well-mixed gas and dust at the same temperature and find that, under such assumptions, we do not reproduce our observations. This argues for the need for additional gas heating mechanisms which may come in the form of X-ray and UV heating. The importance of UV and X-ray heating in the surface layers of disks has been demonstrated observationally by Bary et al. (2003) and Qi et al. (2006).

The procedure used to derive a temperature of $T = 670 \pm 40$ K and mass of $M = 0.52 \pm 0.15 M_{\oplus}$ from a simultaneous fit to the H₂ S(1), S(2), and S(4) lines assumes the gas is optically thin and in LTE at a single temperature. If the emission arises in the atmosphere of a disk where radial and vertical temperature gradients exist, the derived temperature should be considered a characteristic or average temperature. In fact, Figure 2 shows evidence that the emission arises in gas at a mix of temperatures. It should be noted that radial temperature gradients in a disk also affect the detectability of various lines. Since we are most sensitive to narrow emission lines, the S(1) line, originating in cooler gas farther out in the disk, is easier to detect than emission in the S(4) line. Emission arising very close to the star from the inner rim of the disk would be more difficult for us to detect at our high spectral resolution due to line broadening.

Our derived temperature, 670 K, is in agreement with the temperature found by Richter et al. (2002) who derived $T > 380$ K based on S(2) and the upper limit on S(1). Brittain et al. (2003) made observations toward AB Aur at $4.7 \mu\text{m}$ of ¹²CO $v = 1-0$ emission. The low-J lines in the resulting population diagram have a steeper slope, interpreted as emission coming from cooler gas than the high-J lines. Fits to the population diagrams assuming LTE gas give $T = 70$ K for the cool gas and $T = 1540$ K for the hot gas. The authors explain the hot CO emission as coming from the inner rim of the disk, while the cool emission originates in the outer flared part of the disk after it emerges from the inner rim's shadow. Blake & Boogert (2004) also observed $4.7 \mu\text{m}$ CO emission from AB Aur. Isothermal fits with $T \sim 800$ K are able to reproduce their line fluxes. The line widths for the CO lines are generally broader than what we observed, suggesting that the CO emission comes from smaller radii or outflowing gas (Blake & Boogert 2004).

Our derived mass, $0.52 M_{\oplus}$, is four orders of magnitude less than the total disk mass of AB Aur (Semenov et al. 2005). This is partly due to the fact that AB Aur's disk is optically thick at mid-infrared wavelengths (Sheret et al. 2003). Most of the gas in the disk is hidden by optically thick dust and is also too cool to emit at our wavelengths. The mass we derive should therefore be interpreted as a lower limit to the amount of warm gas on the surface of the disk facing us.

By comparing the FWHM of our observed S(2) line profile with computed line profiles from a simple Keplerian disk model, we derive an estimate of where the line emission originates. We generate line profiles under the assumption of emission from a Keplerian disk inclined at 17° (Semenov et al. 2005) orbiting a $2.4 M_{\odot}$ star (van den Ancker et al. 1998) with equal emissivity at all points within an annulus 2 AU in extent. We convolve the line profiles with our instrumental broadening function plus a thermal broadening function based on our derived temperature, $T = 670$ K, and compare the resulting FWHM of the line profiles to our observed S(2) line. Under these assumptions, the line profiles imply that our emission arises near 18 AU in the disk.

We used parameters for the disk based on the fit to AB Aurigae's SED from Dullemond et al. (2001) as input to the vertical disk structure model of Dullemond et al. (2002) in order to derive a grid of temperature and density values as a function of disk radius and height above the midplane. The Dullemond et al. (2001) model does an excellent job fitting the SED, although we note that their derived inclination angle, 65° , is significantly larger than our assumed value of 17° . As noted in Dullemond et al. (2001), the large discrepancy between their derived inclination and what most observations suggest is probably due to the inclusion in their SED model of a perfectly vertical inner rim which may not be physically accurate. We input this radial and vertical temperature and density profile into an LTE radiative transfer program. We assume the gas is in LTE with the dust and compute the emergent spectrum. The emission lines produced by our model under these conditions are much weaker than our observations. This is not especially surprising given our assumption of well-mixed gas and dust at the same temperature and suggests the need for additional gas heating mechanisms.

The vertical structure model of Dullemond et al. (2002) is mainly concerned with modeling the dust emission from disks. By assuming equal gas and dust temperature, the gas only reaches a temperature of ~ 260 K at the top of the disk at 18 AU, much cooler than our derived temperature of 670 K. To explain the observed emission, an additional mechanism is needed to heat the gas. X-ray and UV heating are likely possibilities which can heat the gas to temperatures significantly hotter than the dust. Glassgold et al. (2007) computed the gas temperature in X-ray irradiated disks around T Tauri stars. At 20 AU, the temperature can reach over 3000 K at the top of the disk before dropping to 500-2000 K in a transition zone and then to much cooler temperatures deep in the disk. Nomura & Millar (2005) considered UV heating of protoplanetary disks and the resulting molecular hydrogen emission. The temperature in their model at 10 AU reaches over 1000 K and predicts an H₂ S(2) line flux of 2×10^{-15} ergs s⁻¹ cm⁻², somewhat lower than our observed flux, but their model was for a less massive star and disk. H₂ emission could also arise in regions where there is spatial separation of the gas from the dust due to dust settling or coagulation of dust into larger particles. The SED of AB Aur shows no evidence for gaps in the AB Aur disk and we are unable to make definitive statements based on our observations.

A UV-heated H₂ layer in a protostellar disk ought to exhibit at least some similarities to the comparable hot

layer at the surface of photodissociation regions (PDRs) with high densities and strong radiation fields. We therefore compare our observations of AB Aur with earlier mid-IR H₂ spectroscopy of the Orion Bar PDR. The UV field expressed in terms of the mean interstellar radiation field that was adopted by Allers et al. (2005) (3×10^4) is somewhat smaller than that expected at 18 AU around an A0 star ($\sim 10^5$). Jonkheid et al. (2007) have computed the strength of the UV field throughout a disk around a Herbig Ae star finding values between $10^5 - 10^6$ near the disk surface at 20 AU. Our derived temperature, 670 K, is in the range of temperatures (400-700 K) derived for the Orion bar PDR based on the H₂ S(1), S(2), and S(4) lines (Allers et al. 2005). As shown in Allers et al. (2005), the line ratios are determined by a complex mix of the temperature gradient, H₂ abundance and dust properties. As another check of the plausibility that the surface of AB Aur's disk is similar to a PDR, we computed the surface brightnesses of our three lines. Assuming our observed emission arises from an annulus 2 AU in extent centered at 18 AU, we derive surface brightnesses of $\sim 10^{-5}$ ergs cm⁻² s⁻¹ sr⁻¹, roughly an order of magnitude lower than those seen by (Allers et al. 2005). However, Allers et al. (2005) estimated that

their line intensities were brightened by a factor of 10 since the Orion Bar PDR is seen nearly edge-on making our surface brightnesses consistent with each other.

We thank the Gemini staff, and John White in particular, for their support in getting TEXES to work on Gemini North. We thank Rob Robinson for useful discussions on the analysis of our data. The development of TEXES was supported by grants from the NSF and the NASA/USRA SOFIA project. Modification of TEXES for use on Gemini was supported by Gemini Observatory. Observations with TEXES were supported by NSF grant AST-0607312. This work is based on observations obtained at the Gemini Observatory, which is operated by the Association of Universities for Research in Astronomy, Inc., under a cooperative agreement with the NSF on behalf of the Gemini partnership: the National Science Foundation (United States), the Particle Physics and Astronomy Research Council (United Kingdom), the National Research Council (Canada), CONICYT (Chile), the Australian Research Council (Australia), CNPq (Brazil) and CONICET (Argentina).

REFERENCES

- Allers, K.N., Jaffe, D.T., Lacy, J.H., Draine, B.T., & Richter, M.J. 2005, ApJ, 630, 368
- Bary, J.S., Weintraub, D.A., & Kastner, J.H. 2003, ApJ, 586, 1136
- Beckwith, S.V.W., Sargent, A.I., Chini, R.S., & Guesten, R. 1990, AJ, 99, 924
- Blake, G.A., & Boogert, A.C.A. 2004, ApJ, 606, L73
- Brittain, S.D., Rettig, T.W., Simon, T., Kulesa, C., DiSanti, M.A., & Dello Russo, N. 2003, ApJ, 588, 535
- Chen, C.H., & Jura, M. 2003, ApJ, 591, 267
- Dullemond, C.P., Dominik, D. & Natta, A. 2001, ApJ, 560, 957
- Dullemond, C.P., van Zadelhoff, G.J. & Natta, A. 2002, A&A, 389, 464
- Fuente, A., Martín-Pintado, J., Rodríguez-Fernández, N.J., Rodríguez-Franco, A., De Vicente, P., & Kunze, D. 1999, ApJ, 518, L45
- Glassgold, A.E., Najita, J. & Igea, J. 2004, ApJ, 615, 972
- Glassgold, A.E., Najita, J. & Igea, J. 2007, ApJ, 656, 515
- Gorti, U. & Hollenbach, D. 2004, ApJ, 613, 424
- Hernández, J., Calvet, N., Briceño, C. Hartmann, L., & Berlind, P. 2004, AJ, 127, 1682
- Johns-Krull, C.M., Valenti, J.A., & Linsky, J.L. 2000, ApJ, 539, 815
- Jonkheid, B., Dullemond, C.P., Hogerheijde, M.R., & van Dishoeck, E.F. 2007, A&A, 463, 203
- Lacy, J.H., Richter, M.J., Greathouse, T.K., Jaffe, D.T., & Zhu, Q. 2002, ApJ, 114, 153
- Mannings, V., & Sargent, A.I. 1997, ApJ, 490, 792
- Meeus, G., Waters, L.B.F.M., Bouwman, J., van den Ancker, M.E., Waelkens, C., Malfait, K. 2001, A&A, 365, 476
- Najita, J., Carr, J.S., & Mathieu, R.D. 2003, ApJ, 589, 931
- Najita, J.R., Carr, J.S., Glassgold, A.E., Valenti, J.A. 2006, in *Protostars and Planets V*, ed. B. Reipurth, D. Jewitt, K. Keil. (Tucson: University of Arizona Press), 507
- Nomura, H., & Millar, T.J. 2005, A&A, 438, 923
- Pascucci, I. et al. 2006, ApJ, 651, 1177
- Qi, C., Wilner, D.J., Calvet, N., Bourke, T.L., Blake, G.A., Hogerheijde, M.R., Ho, P.T.P., & Bergin, E. 2006, ApJ, 636, L157
- Richter, M. J., Jaffe, D. T., Blake, G. A., & Lacy, J. H. 2002, ApJ, 572, L161
- Roberge, A. et al. 2001, ApJ, 551, L97
- Semenov, D., Pavlyuchenkov, Y., Schreyer, K., Henning, T., Dullemond, C., & Bacmann, A. 2005, ApJ, 621, 853
- Sheret, I., Ramsey Howat, S.K., & Dent, W.R.F. 2003, MNRAS, 343, L65
- Thi, W.F. et al. 2001, ApJ, 561, 1074
- van den Ancker, M.E., de Winter, D., & Tjin A Djie, H.R.E. 1998, A&A, 330, 145

TABLE 1
OBSERVING PARAMETERS

Date	Telescope	Line ^a	Resolving Power ^b ($R \equiv \lambda/\delta\lambda$)	Slit Width ^c (arcsec, AU)	Integration Time (s)
Dec 2002	IRTF	S(1)	60,000	2.0, 288	2591
Dec 2002	IRTF	S(2)	85,000	1.4, 202	4792
Dec 2003	IRTF	S(2)	81,000	1.4, 202	2072
Oct 2004	IRTF	S(4)	88,000	1.4, 202	8549
Nov 2006	Gemini	S(1)	80,000	0.81, 117	2007
Nov 2006	Gemini	S(2)	100,000	0.54, 78	2072
Nov 2006	Gemini	S(4)	100,000	0.54, 78	1295

^aS(1) is at 587.0324 cm⁻¹. S(2) is at 814.4246 cm⁻¹. S(4) is at 1246.098 cm⁻¹.

^bThe resolving power is deduced from observations of stratospheric emission from Titan or Saturn at similar frequencies or unresolved emission lines in a low pressure gas cell.

^cThe slit width in AU is calculated at AB Aur's distance of 144 pc.

TABLE 2
SUMMARY OF RESULTS

Telescope	λ (μm)	F_ν (Jy)	Line Flux (10^{-14} ergs s^{-1} cm^{-2})	Equivalent Width (km s^{-1})	FWHM (km s^{-1})
IRTF	8	12.9 (1.1)	< 1.2
	12	13.3 (0.4)	0.93 (0.25)	0.86 (0.23)	7.0
	17	25.2 (1.8)	< 1.1
Gemini	8	12.7 (0.4)	1.47 (0.34)	0.93 (0.21)	10.4
	12	14.7 (0.3)	0.53 (0.07)	0.44 (0.06)	8.5
	17	24.6 (0.4)	1.1 (0.30)	0.76 (0.21)	9.0

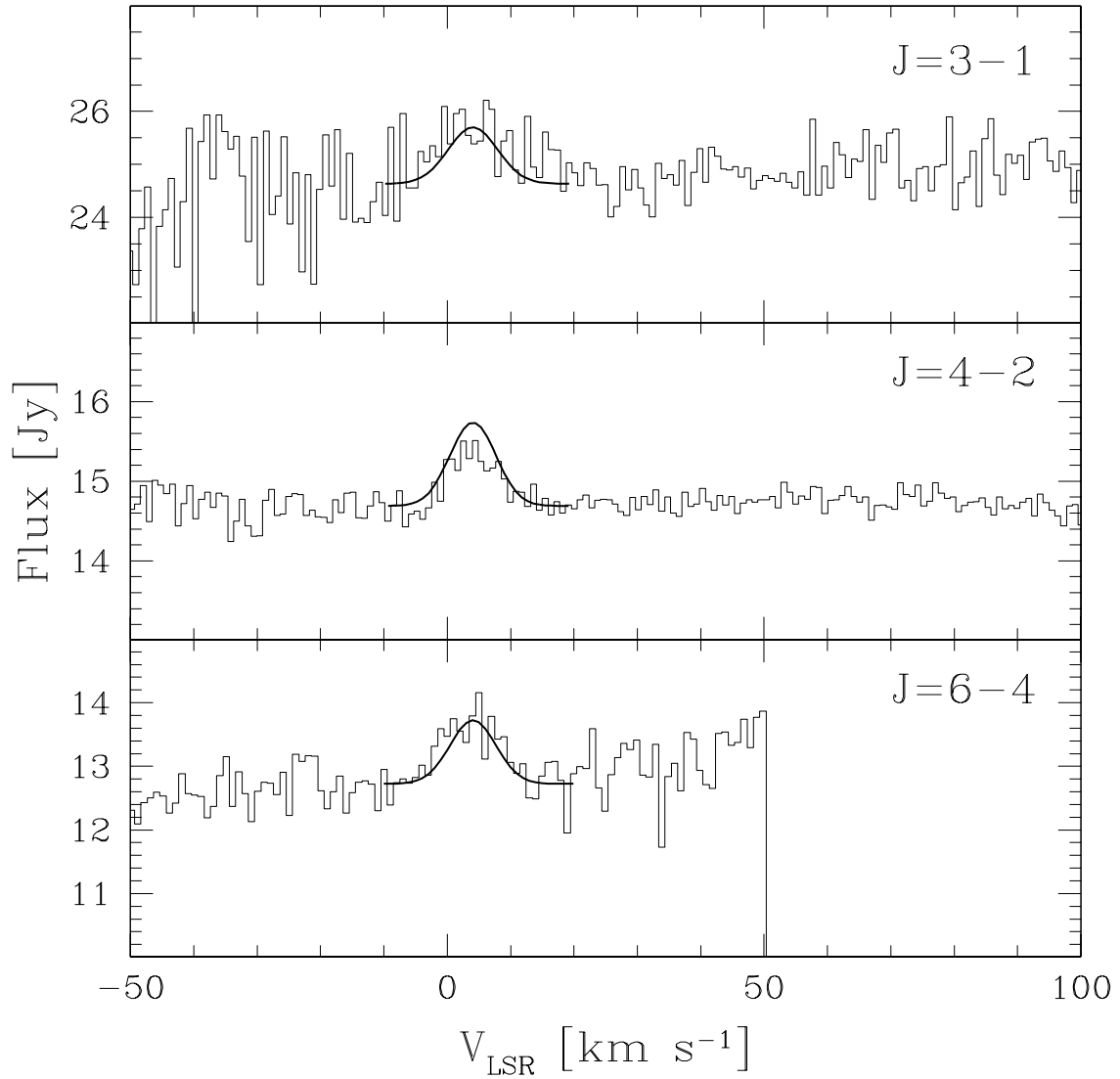


FIG. 1.— Regions of the three H₂ pure rotational lines available from the ground. The data shown were obtained at Gemini North in November 2006 under Gemini program GN-2006B-Q-42. Each spectrum has been flux-calibrated. The lines were individually fit with a Gaussian to determine their centroid, flux, and FWHM. The lines are all centered near the systemic velocity of AB Aur and have FWHM ~ 10 km s⁻¹. Line fluxes are listed in Table 2. The overplotted Gaussians are based on the simultaneous fit and are not the individual fits to each line. The three spectral regions were simultaneously fit with a model assuming the observed emission arises from a mass of H₂ gas at a single temperature. The best-fit model with $T = 670$ K and H₂ mass = $0.52 M_{\odot}$ is overplotted.

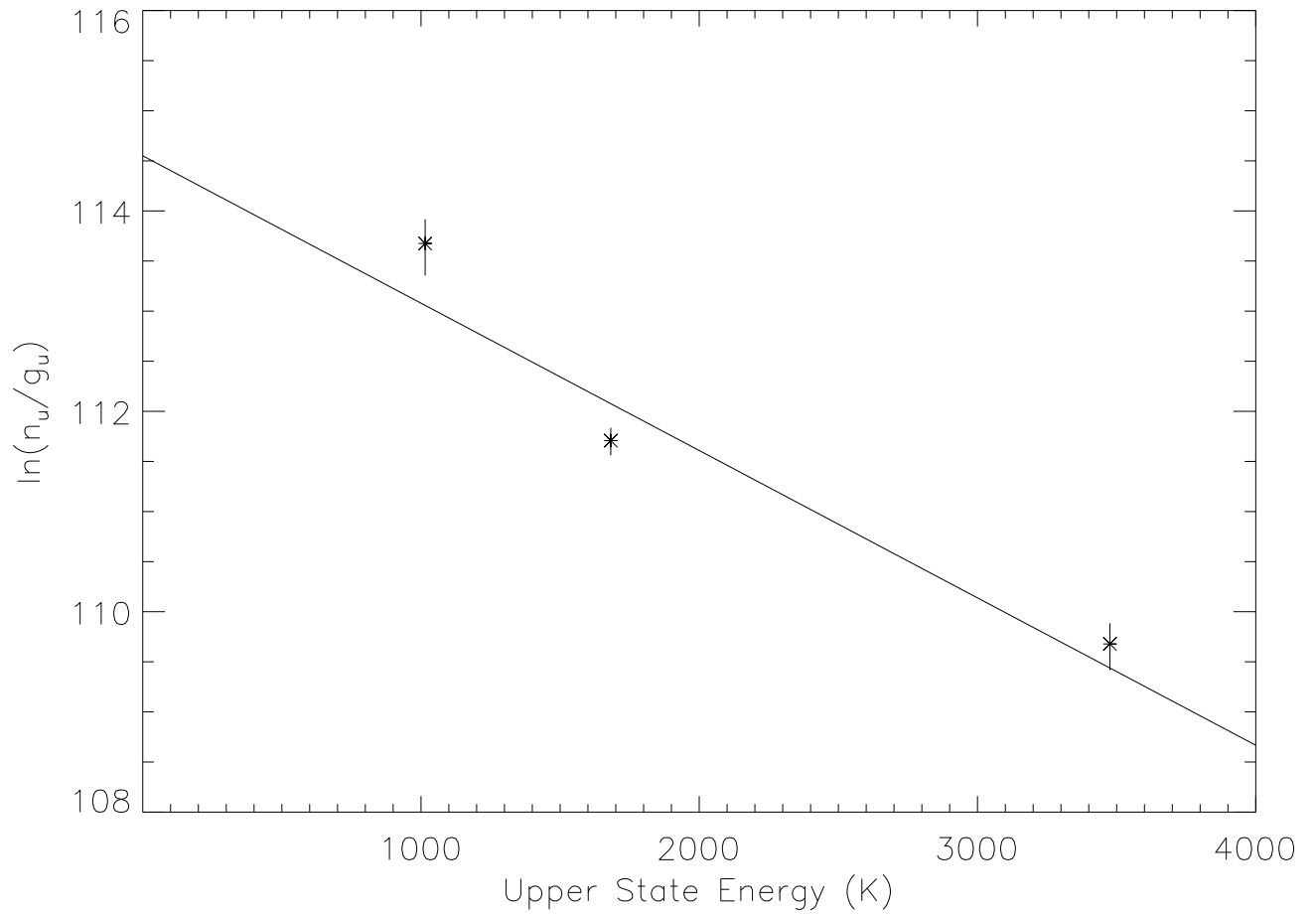


FIG. 2.— Population diagram based on Gemini North observations. The points marked are based on fluxes derived by fitting a Gaussian to each of the lines and shown with $1-\sigma$ error bars. The overplotted solid line is not a fit to the population diagram; rather it is based on the best-fit model temperature and mass found by simultaneously fitting all three lines. The deviation of the points from the single-temperature line is significant and suggests that the emission may arise from gas at a range of temperatures.